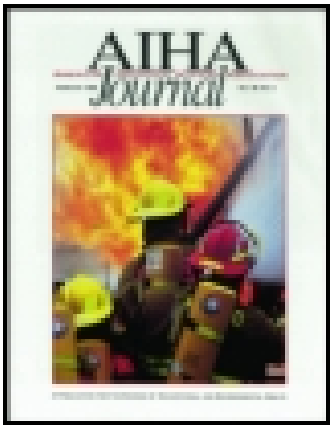

American Industrial Hygiene Association Journal
Publication details, including instructions for authors and subscription information:
http://www.tandfonline.com/loi/aiha20

Multicellular Model for Contaminant Dispersion and Ventilation Effectiveness with Application for Oxygen Deficiency in a Confined Space

CHULHONG PARK [a] & RICHARD P. GARRISON [a]
[a] School of Public Health, The University of Michigan, Ann Arbor, MI 48109
Published online: 04 Jun 2010.

Am. Ind. Hyg. Assoc. J. 51(2):70-78 (1990)

Multicellular Model for Contaminant Dispersion and Ventilation Effectiveness with Application for Oxygen Deficiency in a Confined Space*

CHULHONG PARK AND RICHARD P. GARRISON†
School of Public Health, The University of Michigan, Ann Arbor, MI 48109

Multicellular models were developed to predict contaminant dispersion in a three-dimensional (3-D) space. The method utilized in this study was patterned after models which have been developed for water pollution in lakes and streams. This approach involved (1) design of cell structures to accommodate the geometry and mass flow characteristics of the 3-D space and (2) approximation of dispersion coefficients to describe contaminant transport in addition to that resulting from mass flow between cells. The dispersion model utilized a mass balance equation to predict contaminant dispersion as a function of time. The computer model was evaluated against experimental data for oxygen deficiency inside a ventilated confined space (CS) model. Eight test cases of ventilation design for the CS model were tested for each of three contaminant release (nitrogen to cause oxygen deficiency) characteristics: (1) purging (oxygen recovery from an initial deficiency); (2) steady state; and (3) variable rate. The dispersion model did a reasonably good job of predicting oxygen concentrations for different locations (cells) in the CS model. The primary limitations of this multicellular method are associated with experimental approximations of flow patterns and dispersion coefficients.

Dilution ventilation can be an effective engineering control method for reducing concentrations of airborne contaminants. It involves the introduction of fresh air and removal of contaminated air within the ventilated space. In some cases, it can be effected by natural air movement. In many cases, especially when hazardous contaminants are involved, mechanical ventilation should be provided.

The conventional dilution ventilation equations have been used for many years to aid in ventilation design.[1] These relationships provide ventilation approximations for steady-state and time-dependent contaminant concentration. They are, however, very limited in their ability to account for variations in contaminant concentration and ventilation effectiveness caused by airflow patterns which change with the geometric configuration of the ventilation inlet(s) and outlet(s) and of the space itself.

The dilution ventilation equations incorporate a "K factor" which serves two functions. One function is to approximate the effectiveness of fresh air mixing with contaminated air, i.e., to serve as a "mixing factor" representing dilution ventilation effectiveness. The other function is to apply a safety factor, prescribing some degree of overdesign to increase ventilation flow rate with increasing risk of contaminant exposure caused by conditions such as contaminant toxicity and nonuniform evolution, work practices, and variable numbers and locations of workers. It is important to emphasize that dilution ventilation generally should not be used for highly toxic contaminants.

This dual function for a single K factor is confusing and sometimes misunderstood. Design applications are confounded by a lack of specific guidelines for selecting either mixing or safety factors. Sources describe K values to have different ranges—for example, from K = 3 to K = 10[1] and from K = 2 to K = 4.[2] The need for data on K factors, especially relative to air mixing and ventilation effectiveness, has been described as the major problem in using the dilution equations and represents a challenge for improvement in ventilation design practices.[2]

The dilution ventilation equations describe a single contaminant concentration throughout the entire ventilated space. This is not true for many situations, however. A previous study[3] has shown that the concentrations were not uniformly distributed in a confined space (CS) model. The dilution ventilation equations may be thought of as single-cell models to approximate ventilation effects. It is reasonable to expect that nonuniform concentration distributions and variable flow patterns can be represented more accurately by multicellular ventilation models.

The objectives of this study were to (1) develop multicellular computer models for contaminant dispersion in a confined space, and (2) evaluate the multicellular models against experimental data for oxygen deficiency in a CS model. The study presented here was part of a research project funded by the National Institute for Occupational Safety and Health (NIOSH) to test,

*The study presented here was part of a research project funded by the National Institute for Occupational Safety and Health (NIOSH) to test, evaluate, and develop useful information on ventilation for work in confined spaces.

†Author to whom correspondence should be addressed.

evaluate, and develop useful information on ventilation for work in confined spaces.

Multicellular Modeling

A three-dimensional (3-D) space can be divided into a number (N) of subspaces or cells, thereby creating a multicellular model of the space. Contaminant movement inside the space can be represented as a group of N cells which interact across cell boundaries. Multicellular models assume instantaneous uniform mixing of contaminant within each cell.

Multicellular models have been used to predict contaminant concentrations and ventilation effectiveness in room and workplace environments.[4-7] These ventilation models typically involved simple flow patterns and a relatively small number of cells. Multicellular models also have been developed for predicting contaminant concentration in lakes and streams.[8,9] These hydraulic models typically involved more cells than for room air models because more cells were needed to represent relatively complex space geometry and water flow patterns.

Contaminants are transported within a 3-D space by mass flow (advection) and dispersion.[10,11] Dispersion occurs as a result of mechanical dispersion (turbulent mixing/convective diffusion) and molecular diffusion (concentration gradient). For this study, dispersion was treated as a general effect causing changes in contaminant concentration between cells in addition to the changes caused by mass flow.

Figure 1 illustrates the concept of contaminant dispersion between cells in a multicellular model. For a typical cell (i), the rate of change of concentration can be described by the following mass balance equation.

$$V_i \frac{dC_i}{dt} = W_i + \sum_{j=1}^{N} Q_{ji} C_j - \sum_{j=1}^{N} Q_{ij} C_i - \sum_{j=1}^{N} D_{ij} A_{ij} \frac{C_i - C_j}{L_{ij}}$$

where V_i = volume of cell i in m^3 (ft^3)
C_i = contaminant concentration in cell i in percent (%)
C_j = contaminant concentration in cell j
W_i = contaminant generation rate in cell i in $\%m^3/sec$ ($\%ft^3/sec$)
Q_{ji} = volume flow rate from cell j to cell i in m^3/sec (ft^3/sec)
Q_{ij} = volume flow rate from cell i to cell j
D_{ij} = dispersion coefficient between cell i and cell j in m^2/sec (ft^2/sec)
A_{ij} = cross-sectional area between cell i and cell j in m^2 (ft^2)
L_{ij} = distance between cell i and cell j in m (ft)
t = time in seconds
N = number of cells

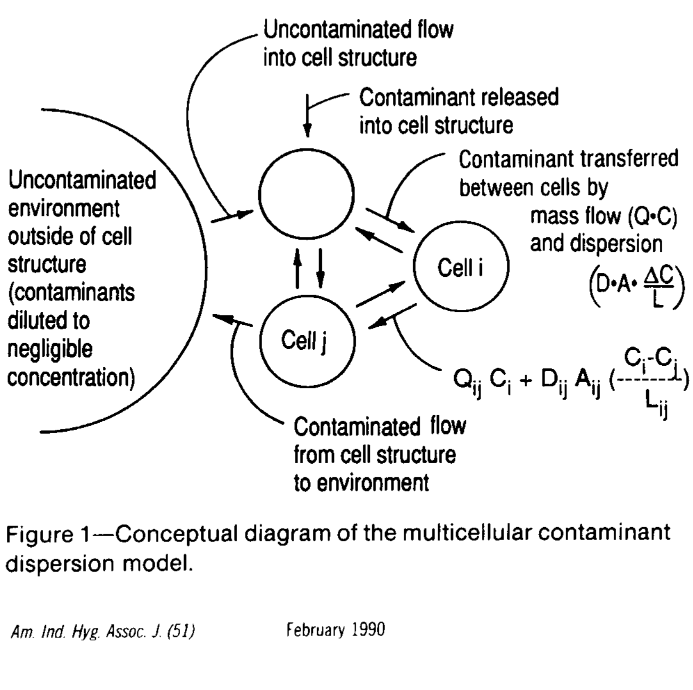

Figure 1—Conceptual diagram of the multicellular contaminant dispersion model.

This model assumes that reactions of contaminants and buoyancy effects are negligible inside the 3-D space. This model is an Nth-order system of first-order, initial-value problems. In this study, the Euler method was used to solve the mass balance equation for time-dependent situations and the Gauss-Seidel iterative method was used for steady-state situations. The model program was written in FORTRAN 77 and run on an IBM-AT personal computer.

Multicellular models can be solved when mass or volume flow rates and dispersion coefficients between cells are specified for a given 3-D space and cell structure. In this study, cell flow rate and dispersion data were obtained by experimental testing.

EXPERIMENTAL FACILITIES AND METHODS

Some confined spaces can be represented by relatively simple geometric configurations. These can include cube-shaped spaces, with a single opening in the top which can be utilized for mechanical ventilation. This particular case was investigated in a previous study on ventilation effectiveness for eliminating oxygen deficiency in a cubical CS model.[3] The basic CS model used for this study was the same as that used for the previous study, except for installation of a new bottom section and different sampling point locations.

Nondimensional units were used to describe total ventilation volume flow rate through the CS model and the elevation of the ventilation inlet/outlet (I/O) opening. Volume flow rate in air changes per hour (ACH) was determined as the actual ventilation volume flow rate divided by the volume of the space (CS model). The I/O elevation was expressed as a percentage of the CS model height (%H) measured from the bottom of the model.

The experimental studies were conducted in two phases: observation of airflow patterns and measurements of oxygen deficiency. Testing of airflow patterns was conducted for eight (2 × 2 × 2) ventilation cases: two modes of ventilation (exhaust and supply), at two volume flow rates (20 and 60 ACH), for two inlet/outlet elevations (25 and 75 %H). Airflow patterns were visualized using smoke tubes attached to a probe. Velocities were measured using a nondirectional thermal probe.

Figure 2 is a photograph of the experimental facility used in this study. It shows the CS model with attendant systems for contaminant (nitrogen) release, ventilation, air sampling and analysis (oxygen concentration, $\%O_2$), and data collection ($\%O_2$ versus time). The CS model was cubical, with a Plexiglas® front and other sides of wood. Each edge of the model was 0.61 m (2.0 ft) in length. A more detailed description of the facility is provided with a previous study.[3]

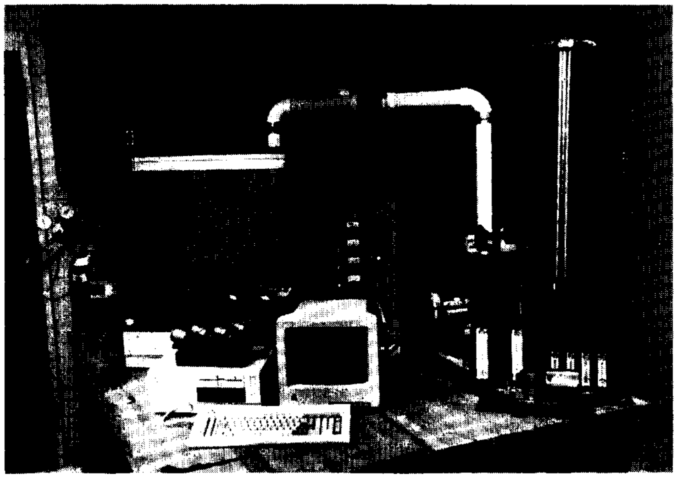

Figure 2—Experimental facility with cubical CS model, ventilation system, sampling system, oxygen monitoring system, nitrogen cylinder, and personal computer.

A new (for this study) bottom section of the CS model was constructed to cause uniform contaminant (nitrogen) release into the model space. It consisted of a sealed wooden plenum containing a closed-loop manifold inside the bottom plenum. The top surface of the plenum (new bottom of CS model) was perforated with numerous holes, 0.3-cm (0.125-in.) in diameter on 2.5-cm (1.0-in.) centers. A quick-throw valve was placed in the nitrogen line for on/off flow control.

The test procedure for measuring oxygen deficiency was the same as in a previous study.[3] An oxygen-deficient atmosphere was created by releasing nitrogen through the bottom of the CS model. Samples of the atmosphere from inside the model were drawn past electrochemical oxygen sensors in a four-channel monitoring system connected to a personal computer. Sampling points were located centrally inside specified cells. Data for each test (%O_2 versus minutes) were collected continuously, with one measurement approximately every second at each location.

The eight ventilation test cases were tested for three types of contaminant release (nitrogen to cause oxygen deficiency): (1) purging (O_2 recovery from an initial deficiency); (2) steady state (constant contaminant release rate); and (3) variable rate (intermittent release). Purging data were used to obtain estimates of dispersion coefficients. This involved iterations (trial and error) of model data using different dispersion coefficients to obtain coefficients which fit the experimental data for purging in each test case. Data from the steady-state and variable-rate conditions were used to evaluate predictions of the multicellular model using the dispersion coefficients obtained from purging.

Figure 3 shows airflow patterns observed for the eight ventilation test cases of this study. It should be noted that a different CS model was used for the airflow studies. The size and shape of the model were the same as for the oxygen-deficiency testing; however, the airflow test model had three clear Plexiglas sides (rather than one) with black-painted interior surfaces to facilitate observation of tracer (white) smoke.

The airflow patterns of Figure 3 illustrate basic characteristics of air movement into, out from, and within the cubical CS model. All flow patterns demonstrated changing directions throughout the space. Within local 3-D regions (cells), however, the flow could be approximated by mass (volume) balance in each cell, with uniform flow across each surface common to another cell. Data to approximate the flow rate between cells were obtained from nondirectional velocity measurements and visual observations of airflow direction (flow patterns) inside the CS model.

Multicellular Models of a Confined Space

The design of multicellular structures for specific applications should address two objectives: (1) to provide adequate detail and accuracy in predicting contaminant dispersion (ventilation effectiveness) and (2) to avoid unnecessary complexity which can limit useful application of the technique. The primary goal in this study was to design a cell structure using the minimum number of cells that could describe the airflow pattern adequately for a specific configuration. The designs of the multicellular structures developed in this study were based on the experimental airflow patterns and subjective consensus of the investigators.

Figure 4 presents top and front views of the four multicellular structures designed for use in this study. The figure shows the exhaust and supply ventilation modes, with high (75 %H) and low (25 %H) inlet/outlet elevations. The top opening in the CS model was a passage for ventilation airflow into and out from the space; it was represented by either one or two cells. The ventilation pipe section was always one cell. The midplane (50 %H) was coincident with cell surfaces in all configurations. Other details and dimensions of cell design varied between configurations.

The region around and below the ventilation pipe experienced the most changes in cell design. The main reason for differences in cell structure between exhaust and supply ventilation was the need to represent the supply "jet" effect by adding one or two cylindrical cells below the ventilation pipe. Symmetry was used to a large extent, as shown in the top views of Figure 4, by using L-shaped cells in all eight configurations.

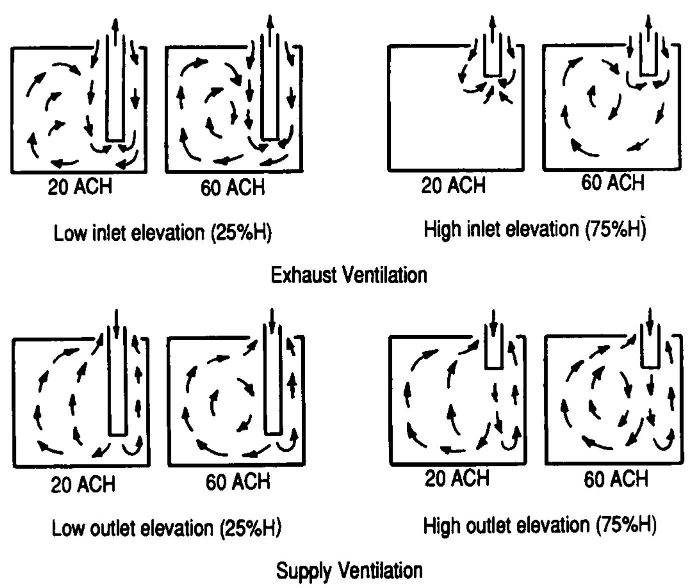

Figure 3—Airflow patterns from tracer smoke studies of the closed-top cubical CS model.

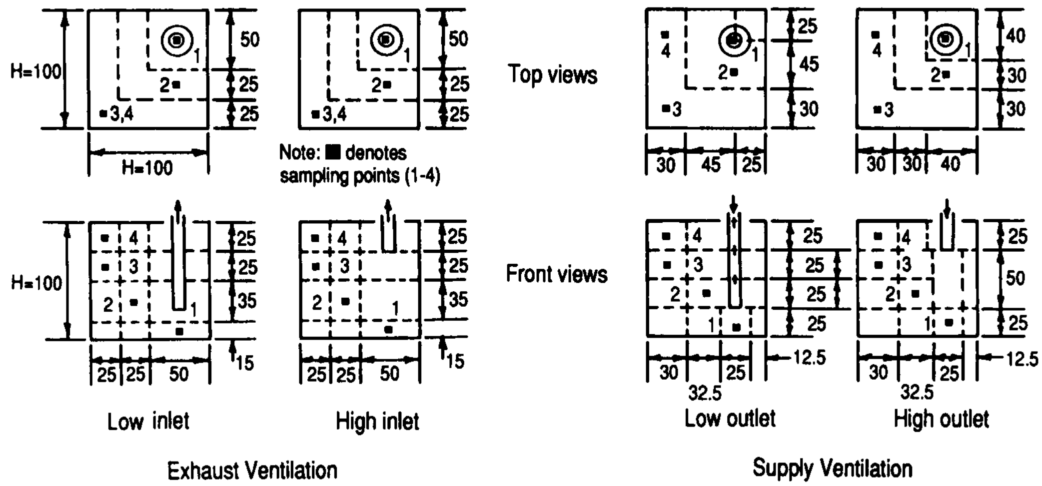

Figure 4—Cell structures and sampling locations for the cubical CS model configurations.

Preliminary studies were conducted in which oxygen concentration was measured at more than one location in a given cell. This testing verified that oxygen levels were symmetrical about the diagonal plane through the ventilation opening and that levels were reasonably uniform within a given cell. Results from a previous study also indicated symmetry in oxygen concentration.[3]

Figure 4 also shows the locations of sampling points. These points were located inside selected cells to provide data for comparison with computer model predictions for the same cells.

Figure 5 is an example of how volume flow rate data between cells were approximated for the dispersion model. This figure shows cell structure and airflow characteristics for exhaust and supply ventilation, with high flow rate (60 ACH) and low inlet (25 %H) and high outlet (75 %H) elevations. Airflow distribution was characterized by the following: (1) mass (volume) balance maintained in each cell, (2) 100 units of flow entering and leaving the CS model, (3) units of flow between cells represented as percentages of the total flow (100 units), and (4) circulatory flow within the CS model approximated relative to the total flow. The flow rate data used in this study were based on the observed airflow patterns and velocity measurements inside the CS model. There was an undeniable aspect of subjective judgment in describing the flowrates shown in Figure 5 and in corresponding data for other configurations. The data used in this study represented the best judgment and consensus of the investigators.

The computer program developed in this study incorporated the multicellular structures and solved the mass balance equation to obtain oxygen concentration as a function of time for each cell. Input data for the computer program included the CS model configuration, the number of cells, the total ventilation volume flow rate (ACH), initial (t = 0) cell concentrations, contaminant release rates into the bottom cells, dispersion coefficients obtained from purging data, volume flow rates between cells, and geometric data including cell volumes, surface areas, and distances to adjacent cells.

EXPERIMENTAL FINDINGS AND DISCUSSION

Figure 6 illustrates effects of variable dispersion coefficients (D) for the four locations selected for experimental testing. The data

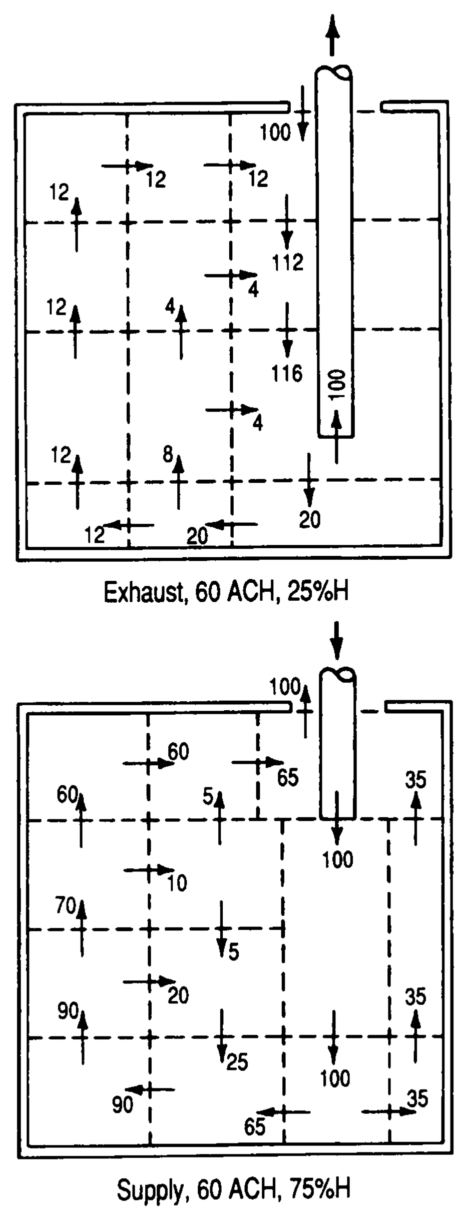

Figure 5—Volume (mass) flow rate approximations between cells for two test cases.

shown are for oxygen recovery (purging) from an initial deficiency for the case of supply ventilation, 60 ACH at 75 %H. Model predictions for D = 0 and D = 0.93 m^2/sec (10 ft^2/sec) are shown for all locations, along with experimental data and predicted oxygen recovery for values of D selected to match closely with the experimental data (every second point plotted). Curves for D = 0 represent contaminant transport by mass flow alone (without dispersion), for which oxygen recovery varies with location. Curves for D = 0.93 m^2/sec (10 ft^2/sec) represent a high rate of contaminant dispersion, which significantly exceeds contaminant transfer caused by mass flow. The curves for D = 0.93 m^2/sec (10 ft^2/sec) were very nearly the same (within 0.02 $\%O_2$) for all locations, thereby approximating complete uniform mixing throughout the space.

The procedure for determining D for each location was by trial and error, knowing that D would fall between 0–0.93 m^2/sec (0 and 10 ft^2/sec) for the multicellular models used in this study. Values of D for Figure 6 were selected to produce curves that were qualitatively (visually) "close" to the experimental data for each of the four selected cells. Indeed, it is possible that other values of D could have provided even closer predictions. The determination of D values which vary for different cells is very complicated because each value of D between any two cells will affect contaminant dispersion for all of the other cells. It may be possible to develop a computer program to obtain optimum values of D, but this was not done in this study.

A modeling procedure utilizing different dispersion coefficients for different locations (cells) may be too complex for practical application. For this preliminary study, it was desirable to simplify the procedure by using a single value of D throughout the model space, accepting the fact that some accuracy would be lost. It should be noted that a single dispersion coefficient may not be appropriate for some situations, such as when interferences cause localized flow patterns and contaminant mixing or when flow is predominantly one- or two-dimensional or when the 3-D space has very complex geometry.

The procedure for selecting a single value of D for each test case was also by trial and error. This involved plotting experimental data and model-predicted curves for different values of D for each selected cell. The final value of D was chosen to be that for which variations of ± 5% failed to produce a closer fit.

Figure 7 presents a comparison of experimental and model-predicted oxygen recovery (purging) using a single value for the dispersion coefficient, D = 0.0019 m^2/sec (0.02 ft^2/sec), for the case of exhaust ventilation, 20 ACH at 25%H. All multicellular model data from this study were obtained using a single value of D.

Figure 7 shows that the experimental data (every second point plotted) had the same general tendencies for oxygen recovery as did the model predictions. The experimental oxygen levels for Location 4 were consistently lower than those for the other locations. The dispersion model predicted nearly the same concentrations for Locations 3 and 4, however, with slightly higher levels for Location 4. This limitation of the dispersion model was believed to result from using a single dispersion coefficient and/or from having less actual airflow in the upper corner of the CS model than was approximated by the volume (mass) flow between cells in the dispersion model. These findings indicated that a single value of D could provide reasonably good predictions of contaminant dispersion and ventilation effectiveness for oxygen recovery in a CS model.

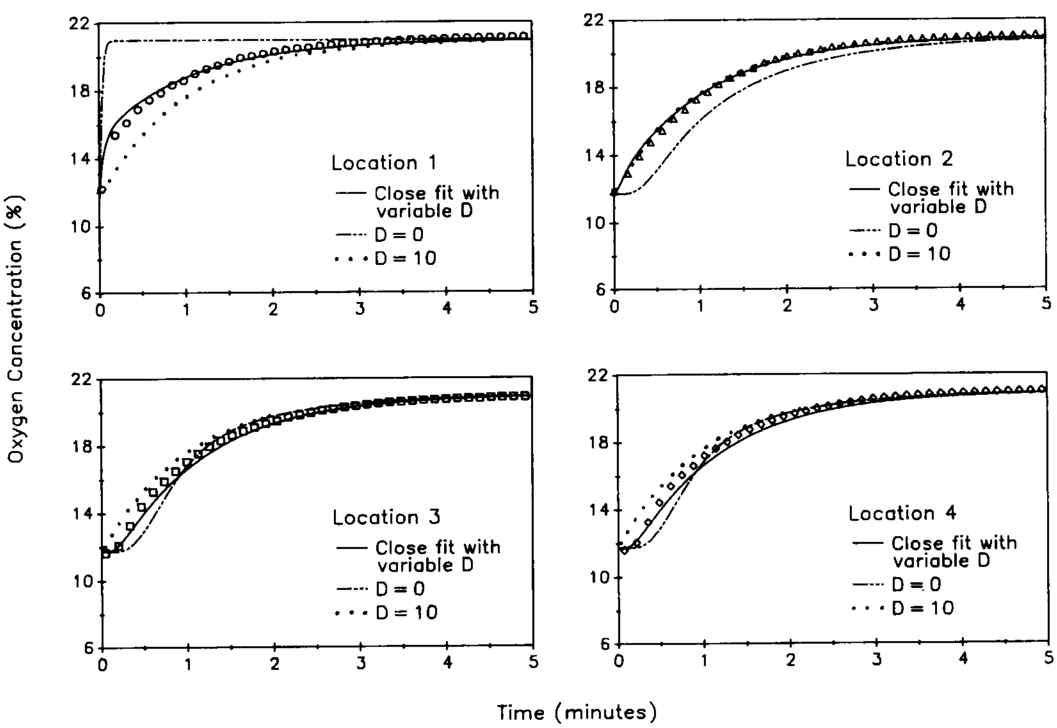

Figure 6—Oxygen recovery (purging) predicted by the dispersion model, with variable dispersion coefficients (D), compared to experimental data for the four sampling locations (supply ventilation, 60 ACH, 75 %H).

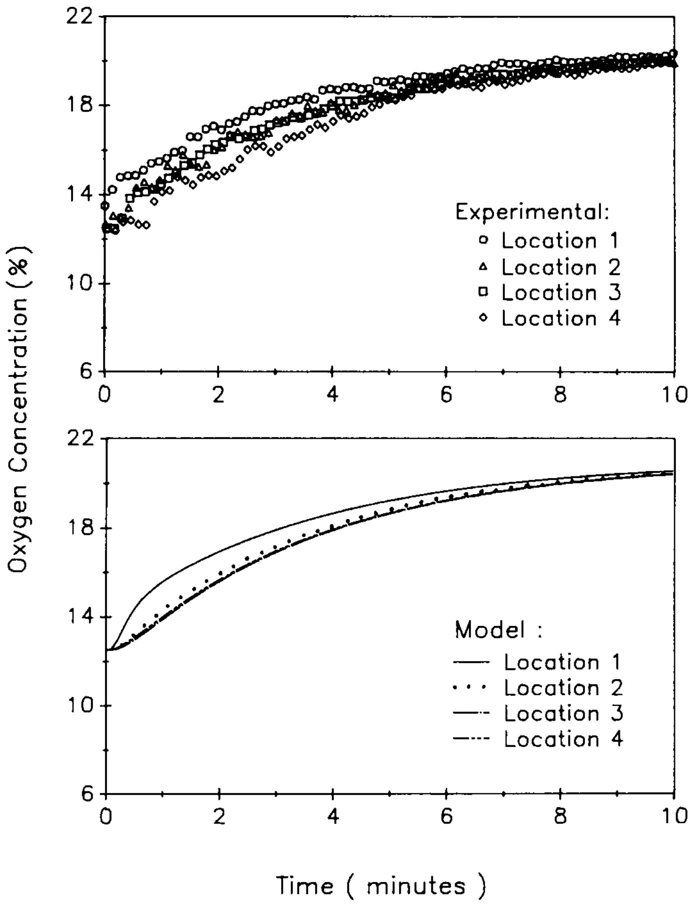

Figure 7—Oxygen recovery (purging) from experimental testing and as predicted by the dispersion model using a single dispersion coefficient, D = 0.02 (exhaust ventilation, 20 ACH, 25 %H).

Figure 8 presents a comparison of model predictions ($\%O_2$) versus experimental results ($\%O_2$) for selected data (every 5th data point) for the eight purging test cases at the four sampling locations. The data are shown to cluster relatively close to the line of "perfect" agreement, i.e., a line with slope of 1.0. Linear regressions of these data produced slopes of 0.996, 1.004, 0.989, and 1.004 for Locations 1, 2, 3, and 4, respectively. Coefficients of determination (R^2) ranged from 90% to 94%, with standard errors (SE) of model estimates ranging from 0.5% to 0.7% (average confidence of 97.0%). For Location 1, the outlying data show that model predictions for initial (first 20 sec) oxygen recovery were much faster than was measured experimentally for supply ventilation, 20 and 60 ACH at 25%H. The greatest variations for all locations occurred for supply ventilation at 25%H, with poorest agreement for 20 ACH. These data indicated good general agreement between dispersion model predictions and experimental findings.

Figure 9 presents comparisons between model predictions and experimental data for steady-state cases of exhaust and supply ventilation at 20 ACH. Nitrogen was released into the CS model at a rate of 10 Lpm. The volume flow rate of contaminant (nitrogen) in these oxygen deficiency tests was significant (2.6 ACH) compared to the ventilation flow rate (20 ACH). It was necessary to include this additional volume flow throughout the cells of the CS model space. If trace contaminants in much lower concentrations and flow rates were being modeled, it might be reasonable to neglect the additional volume of the contaminants being released. This is anticipated to be a subject for further study.

The dispersion model predictions for steady-state oxygen levels generally were close to the experimental data. The steady-state data indicated a trend of consistent variation between model

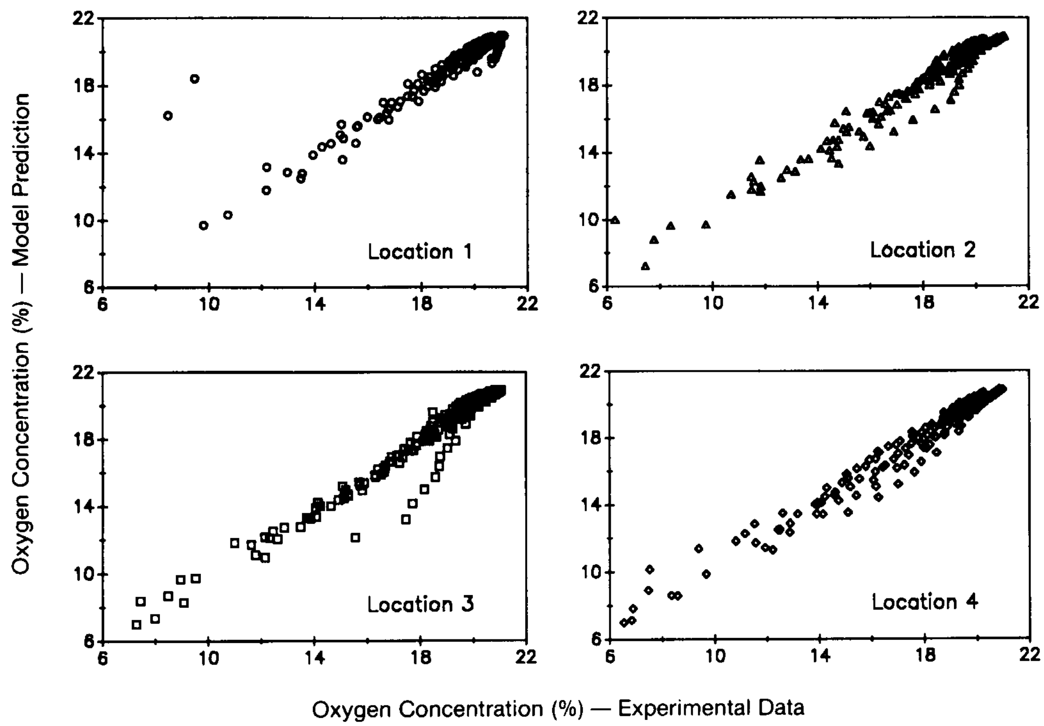

Figure 8—Dispersion model predictions versus experimental data for the eight test cases of oxygen recovery (purging).

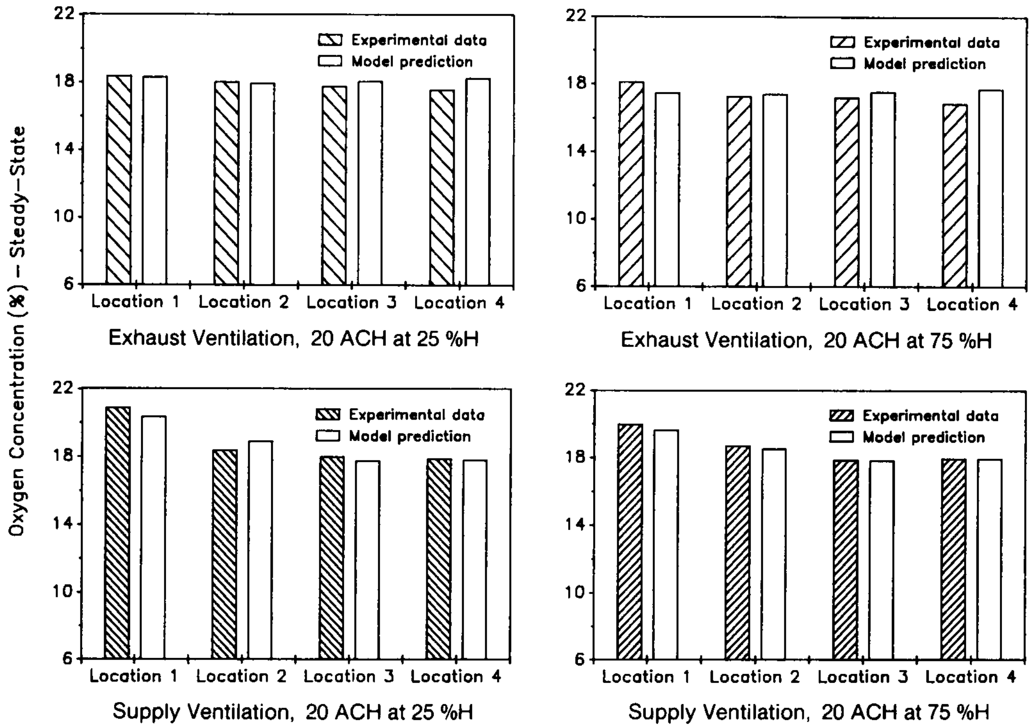

Figure 9—Dispersion model predictions and experimental data for steady-state oxygen concentrations under exhaust and supply ventilation (four cases, 20 ACH).

and experimental data for Locations 1, 2, and 3. Location 1 always had the highest oxygen concentration, with Locations 2 and 3 being relatively close (averaging within 0.2 %O_2). The model predicted slightly higher oxygen levels for Location 4 than for Location 3, but the experimental data generally showed lower oxygen levels. Overall, the model appeared to work reasonably well for the steady-state cases.

For exhaust ventilation, the differences between the model and experimental steady-state oxygen levels generally were within 0.3 %O_2, except for Location 4 for which the differences ranged from 0.8 to 0.9 %O_2. The greater variation at Location 4 (exhaust) may illustrate a limitation of the dispersion model, which did not take buoyancy (nitrogen less dense than air) into account and, thus, could not predict nitrogen accumulation in the upper corner of the CS model.

For steady-state supply ventilation, the model predictions for Locations 3 and 4 were very close to the experimental data (within 0.2 %O_2). This indicated that nitrogen accumulation in the upper corner was not significant for supply ventilation. For Locations 1 and 2, the differences between model and experimental data ranged from 0.2 to 0.5%O_2 and may have been affected by supply airflow interfering with (reducing) nitrogen release from the perforated plenum/bottom of the CS model below the ventilation outlet.

Figures 10 and 11 are comparisons of model predictions and experimental data (every 16th point) for variable contaminant (nitrogen) release rates for the case of supply ventilation, 20 ACH at 75%H. The average rate of nitrogen release (2.5 Lpm) was the same for both figures. The data for Figure 10 were obtained by introducing nitrogen at 5.0 Lpm for 20 min, followed by 20 min with zero release. The data for Figure 11 represent 10.0 Lpm of nitrogen released over 10 min followed by 30 min of no release. Two complete on/off release cycles are shown in the figures.

The dispersion model provided reasonably good predictions of oxygen concentration variation with time for variable contaminant release. Linear regressions of model predicted versus experimental oxygen levels for Figure 10 yielded slopes of 0.994, 1.003, 0.990, and 0.998 for Locations 1, 2, 3, and 4, respectively, with R^2 ranging from 73% to 83% and SE of model estimates ranging from 0.2% to 0.3% (average confidence of 98.5%). Similar regressions for Figure 11 gave slopes of 0.994, 1.000, 0.992, and 1.000 for Locations 1, 2, 3, and 4, respectively, with R^2 ranging from 75% to 90% and SE of model estimates ranging from 0.2% to 0.4% (average confidence of 98.5%).

The slight variations which are evident in Figures 10 and 11 resulted largely from experimental causes. The drop in oxygen levels for the experimental data were not as abrupt as for the model because the plenum below the perforated bottom of the CS model probably became diluted with air during the "off" portion of the cycle so that something less than 100% nitrogen was released into the CS model initially during the "on" portion of the cycle. Also, oxygen recovery during the off portion of the cycle probably was delayed by the same condition, i.e., residual nitrogen from the plenum entering the CS model.

CONCLUSIONS AND RECOMMENDATIONS

The multicellular contaminant dispersion modeling method appeared to work quite well in predicting contaminant concentration within a 3-D space. For the test cases of oxygen deficiency in the CS model used in this study, the dispersion model worked

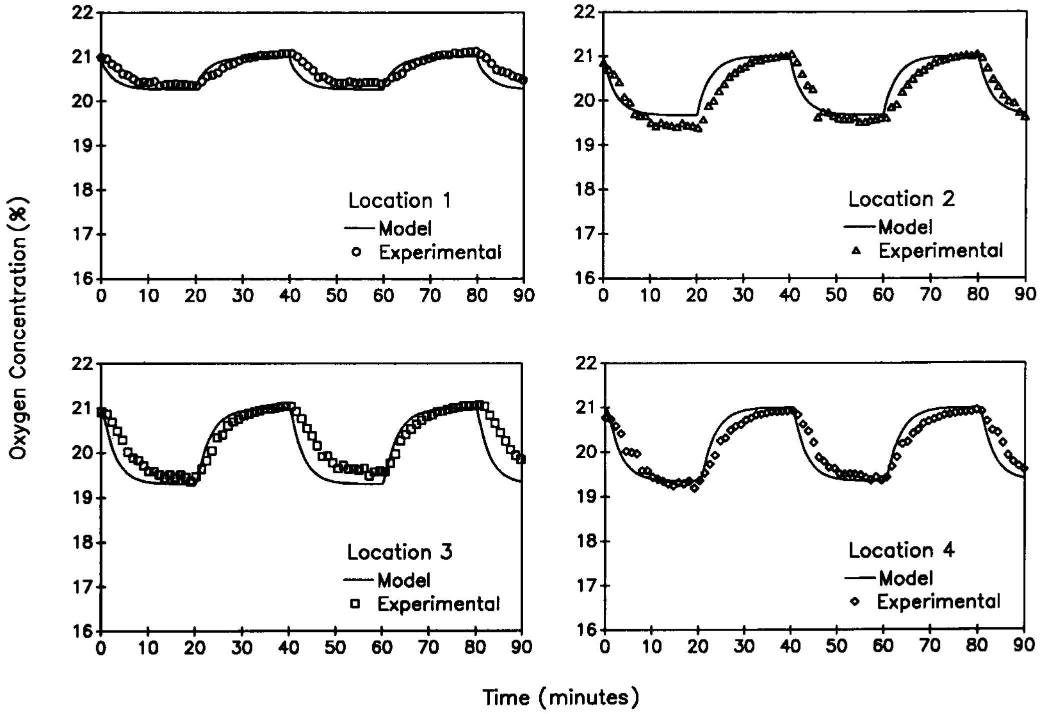

Figure 10—Dispersion model predictions and experimental data for oxygen concentration with a variable rate of nitrogen release, on 20 min and off 20 min (supply ventilation, 20 ACH, 75 %H).

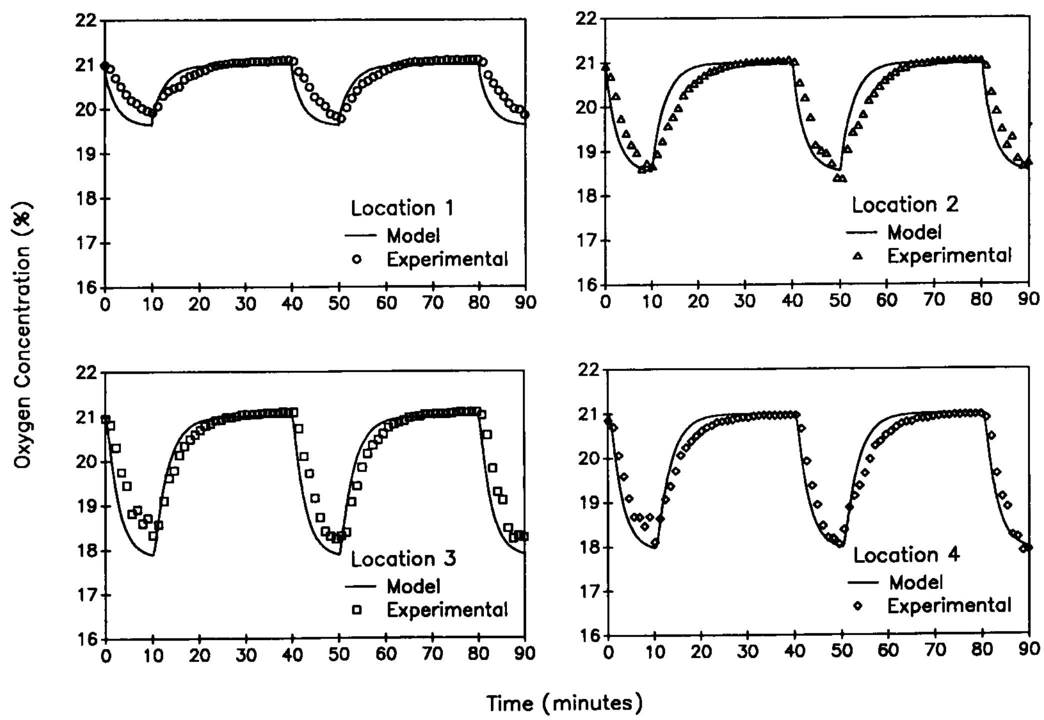

Figure 11—Dispersion model predictions and experimental data for oxygen concentration with a variable rate of nitrogen release, on 10 min and off 30 min (supply ventilation, 20 ACH, 75 %H).

well for different contaminant release characteristics, i.e., purging, steady state, and variable rate. It also would be appropriate to test the model against experimental data for much smaller (trace) amounts of contaminant release. Subsequent studies of this type are planned.

The multicellular modeling approach presented here involved designing a cell structure to accommodate the shape of the 3-D space (CS model) and the patterns of ventilation airflow observed in the test cases. This need for relatively detailed knowledge of the airflow pattern was a significant limitation of the method because such information generally is not available or easily obtained. It is hoped that other computer models someday may provide means to predict airflow patterns with reasonable accuracy and that output from airflow models could be used in development of multicellular dispersion models.

The need for empirical determination of the dispersion coefficient (D) was another limitation. Some experimental data were needed in order to provide the value(s) of D required to apply the multicellular models. In this study, data for the purging situations were used to estimate D and then were applied to steady-state and variable-rate situations. It also should be possible to obtain acceptable values of D from experimental data for either of the other situations. This is another area for further investigation.

The primary advantage of multicellular models is their ability to predict localized contaminant concentrations, which the single-cell dilution models do not. Multicellular dispersion models could be used to estimate K mixing factors used in the conventional dilution ventilation equations. Safety factors still may be needed for designing ventilation requirements for some situations.

This study has shown that a single value of D provided reasonably good predictions for each test case involving oxygen deficiency in a cubical CS model. It is expected that some situations would not favor the use of a single coefficient. These would include localized airflow interferences, flow in only one or two dimensions, and 3-D spaces having complex geometries.

Multicellular models eventually may be applied for actual workplaces. This will require measurements of airflow and determinations of dispersion coefficients in the workplace itself. Alternatively, it may be possible to use smaller, laboratory scale models of the workplace, provided that the smaller models can be verified to have similar airflow and contaminant dispersion characteristics. Future studies could be conducted in this area.

Overall, the multicellular modeling approach appears to have the potential for useful applications in modeling contaminant levels in workplace environments. Further testing of the approach is in order, and coupling of the method with other models to predict airflow patterns could advance the method significantly.

REFERENCES

1. **Mutchler, J.E.:** Principles of Ventilation. In *The Industrial Environment—Its Evaluation and Control.* 2d ed. Washington, D.C.: Government Printing Office, 1973. pp. 578–580.
2. **Kaplan, K.J.:** Research and Development Trends and Needs for Ventilation. In *Ventilation '85. Proceedings of the 1st International Symposium on Ventilation for Contaminant Control, October 1–3, 1985, Toronto, Canada.* New York: Elsevier Science Publishing Co., Inc., 1986. pp. 1–17.
3. **Garrison, R.P., R. Nabar, and M. Erig:** Ventilation to Eliminate Oxygen Deficiency in the Confined Space—Part One: A Cubical Model. *Am. Ind. Hyg. Assoc. J. 4*:1–11 (1989).
4. **Sinden, F.W.:** Multi-Chamber Theory of Air Infiltration. *Build. Environ. 13*:21–28 (1978).
5. **Sandberg, M.:** What Is Ventilation Efficiency? *Build. Environ. 16*:123–135 (1981).
6. **Siren, K.E.:** A Procedure for Calculating Concentration Histories in Dwellings. *Build. Environ. 23*:103–114 (1988).
7. **Waters, J.R. and M.W. Simons:** The Evaluation of Contaminant Concentrations and Airflows in a Multizone Model of a Building. *Build. Environ. 22*:305–315 (1987).
8. **Canale, R.P., S. Nachiappan, D.J. Hineman, and H.E. Allen:** A Dynamic Model for Phytoplankton Production in Grand Traverse Bay. In *Proceedings of the 16th Conference on Great Lakes Research.* Ann Arbor, Mich.: International Association for Great Lakes Research, 1973. pp. 21–33.
9. **Canale, R.P. and J. Squire:** A Model for Total Phosphorus in Saginaw Bay. *J. Great Lakes Res. 2*:364–373 (1976).
10. **Bear, J.:** *Hydraulics of Groundwater.* New York: McGraw-Hill, 1979. pp. 227–239.
11. **Thomann, R.V. and J.A. Mueller:** *Principles of Surface Water Quality Modeling and Control.* New York: Harper & Row, 1987. pp. 71–76, 206–213.